ARTICLE

Theoretical Study of Atomic Structure and Elastic Properties of Branched Silicon Nanowires

Pavel B. Sorokin,[†,‡,⊥,*] Alexander G. Kvashnin,[†] Dmitry G. Kvashnin,[†] Julia A. Filicheva,[†] Pavel V. Avramov,[†,§] Alexander S. Fedorov,[§] and Leonid A. Chernozatonskii[‡]

[†]Siberian Federal University, 79 Svobodny Avenue, Krasnoyarsk, 660041 Russian Federation, [‡]Emanuel Institute of Biochemical Physics, Russian Academy of Sciences, 4 Kosigina Street, Moscow, 119334 Russian Federation, and [§]Kirensky Institute of Physics, Russian Academy of Sciences, Akademgorodok, Krasnoyarsk, 660036 Russian Federation. [⊥]Present address: Department of Mechanical Engineering & Material Science and Department of Chemistry, Rice University, Houston, Texas 77251.

ABSTRACT The atomic structure and elastic properties of Y-shaped silicon nanowires of "fork"- and "bough"-types were theoretically studied, and effective Young moduli were calculated using Tersoff interatomic potential. The oscillation of fork Y-type branched nanowires with various branch lengths and diameters was studied. In the final stages of the bending, the formation of new bonds between different parts of the wires was observed. It was found that the stiffness of the nanowires is comparable with the stiffness of Y-shaped carbon nanotubes.

KEYWORDS: silicon nanowires · elastic properties · molecular mechanics · Tersoff potential

Nanostructures, such as nanocrystals and nanowires (NW), represent the key building blocks for nanoscale science and technology. Nanowires are the most promising elements of nanotechnology. They can be used as field-effect transistors (FETs),[1,2] logic gates,[3] sensors,[4] and more. The effective sizes and electronic properties of the species can be controlled during synthesis in a predictable manner.[5] An ability to obtain perfect silicon nanowires with millimeter length[6] opens new perspectives of using NWs as elements of micromechanical devices. Another perspective technological field is to use branched and hyperbranched nanowires. Conceptually, such structures offer another approach for increasing structural complexity and enable greater functionality. For example, branched NWs might serve as building blocks to design a 3D interconnected computing structure.[7]

Dendrite-like nanowires were obtained by Fonseca *et al.*[8] using the electron-beam-induced approach. Such structures can be treated as the "fork" Y-type branched nanowires (Si−Y−NWs, Figure 1a) with a 90° angle between equal branches. Wang *et al.*[9] proposed a synthetic approach to branched nanowires of various chemical compositions. The single silicon nanowires serve as substrates to deposit gold nanoclusters. After that, a routine technique was used to grow nanowire branches in the same way as the initial wire stem. This method can be used to obtain the "bough" Y-type branched nanowires (Si−YB−NWs, Figure 1b) with a 60° angle between the branches and stem with effective wire diameters from 22 to 30 nm. Alivisatos *et al.* reported a wet synthesis of tetrapod or branched nanocrystals of cadmium telluride and cadmium selenide, controlling the diameter of identical arms.[10]

Though there is a lot of experimental activity, only very limited theoretical studies of the branched nanowires were carried out. In the paper of Menon *et al.*,[11] nanotrees with a stem and perpendicular branches of hypothetical clathrate-like nanowires were investigated and their electronic properties were calculated. The electronic properties of Si nanoflowers were studied by Avramov *et al.*[12] The presence of only two theoretical papers devoted to this topic can be explained by the fact that the smallest realistic models of the branched NWs contain $\sim 10^3$ or more atoms; therefore, a theoretical study of the proposed objects using *ab initio* techniques is a great challenge to quantum chemistry. Until now, *ab initio* methods of quantum chemistry were applied for calculations of elastic properties of only single-crystalline nanowires.[13,14]

Presented here is a theoretical study of atomic structure and mechanical properties of the branched silicon nanowires of fork and bough types using the model Tersoff interatomic potential. Using the ex-

*Address correspondence to psorokin@rice.edu.

Received for review December 10, 2009 and accepted April 13, 2010.

Published online April 22, 2010.
10.1021/nn9018027

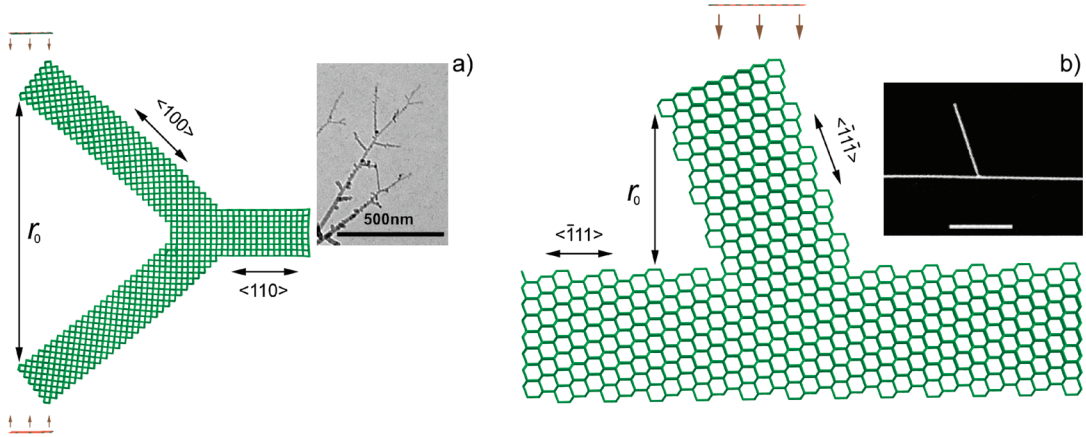

Figure 1. Models of Si−Y−NWs: (a) fork- and (b) bough-types with frozen planes which simulate external pressure. Insets: scanning electron microscopy images of a branched silicon nanowires. Panel a is adapted and reprinted with permission from ref 8. Copyright 2005 American Institute of Physics. The scale bar is equal to 500 nm. Panel b is adapted with permission from ref 9. Copyright 2004 American Chemical Society. The scale bar is equal to 1 μm.

tended cluster models, the effective Young elastic moduli of the junctions were calculated. It was shown that, in contrast to similar Y-junctions of carbon nanotubes, Y-shaped nanowires behave as springs up to direct contact of the branches. The most drastic changes (including formation of new chemical bonds) in the atomic structure of the branched nanowires caused by the external stress are located in the branch crossing region. The unique mechanical properties of the clusters enable their use as structural units of mechanical nanodevices.

Structural Models. Two possible types of three-terminal branched nanowires of finite lengths were studied. The first type (Y fork configuration, Figure 1a) has two equivalent branches attached to the stem. This cluster was used to study the dendrite-like nanowires previously obtained experimentally.[8] Unfortunately, no data concerning the atomic structure of the experimental wires are available. To describe the silicon dendrite structures we chose ⟨110⟩ orientation of the NW stem and ⟨100⟩ orientation of the branches as the most natural structure of the Si−Y−NWs. We assumed that the nanowires form a perfect Si crystal lattice,[15] unpassivated or passivated by hydrogen atom surfaces.

TABLE 1. Elastic Properties of Studied Si−Y−NW[a]

d, Å	L, Å	L_{stem}, Å	$\varepsilon_{critical}$	$\varepsilon'_{critical}$	E'', eV	Y_{eff}, GPa	E''/r_0, eV/Å
13.4	24.7	13.3	0.67	0.68	56.23	1.02	1.71
	36.1	13.4	0.88	0.94	42.82	0.55	0.92
	47.3	13.4	0.83	0.84	34.41	0.33	0.55
	86.8	13.6	0.93	0.97	17.19	0.11	0.19
	110.1	13.7	0.74	0.96	17.63	0.08	0.14
17.3	27.5	15.3	0.43	0.83	327.40	5.98	9.98
	49.6	15.6	0.75	0.88	179.21	1.84	3.07
	68.6	17.5	0.95	0.97	102.05	0.84	1.39
	76.6	9.5	0.94	0.97	112.85	0.77	1.29

[a] The d and L are the wire's branch diameter and length, respectively; L_{stem} is the length of the NW stem; $\varepsilon_{critical}$ is critical strain for re-formation of the chemical bonds in the region of branch crossing; and $\varepsilon'_{critical}$ is critical strain to form new chemical bonds between the branch ends.

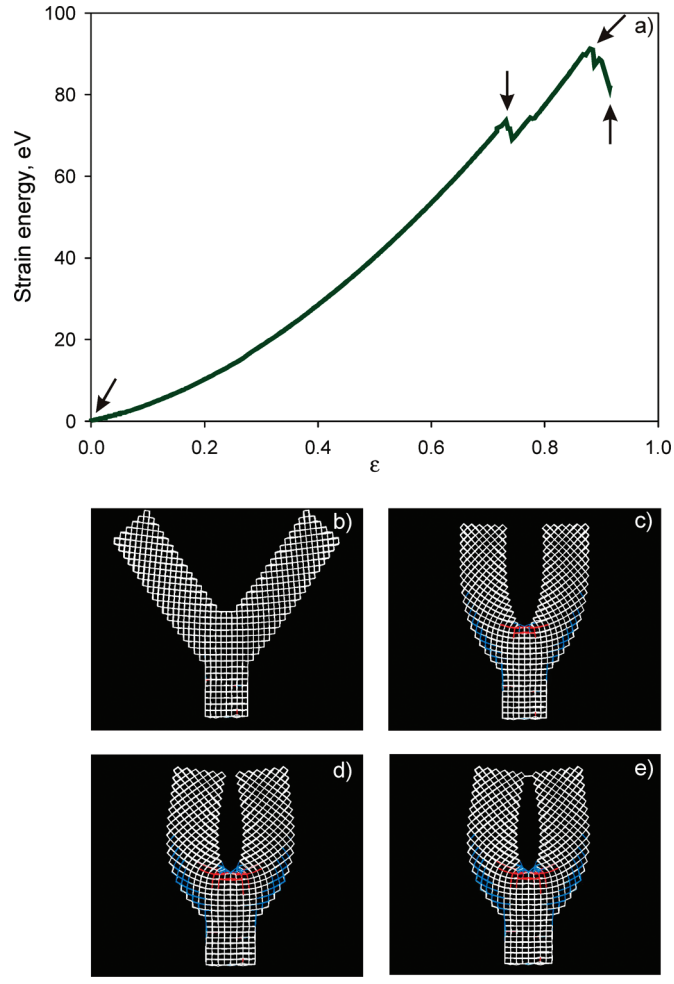

Figure 2. Behavior of a Si−NW fork junction under loading (a) strain energy of the Si−Y−NW (d = 17.3 Å, L = 49.6 Å) as a function of deformation ε. The arrows correspond to the stages of wire compression: (b) unstrained configuration (ε = 0); (c) $\varepsilon_{critical}$ = 0.75; (d) ε = 0.876 before creation of the bonds between the branches; and (e) ε = $\varepsilon'_{critical}$ = 0.879 after creation of the bonds between the branches of the Y−NW. The bonds shown in red have lengths less than 2.26 Å, and bonds shown in blue have lengths more than 2.41 Å (the bond length in the bulk silicon is equal to 2.3516 Å[15]).

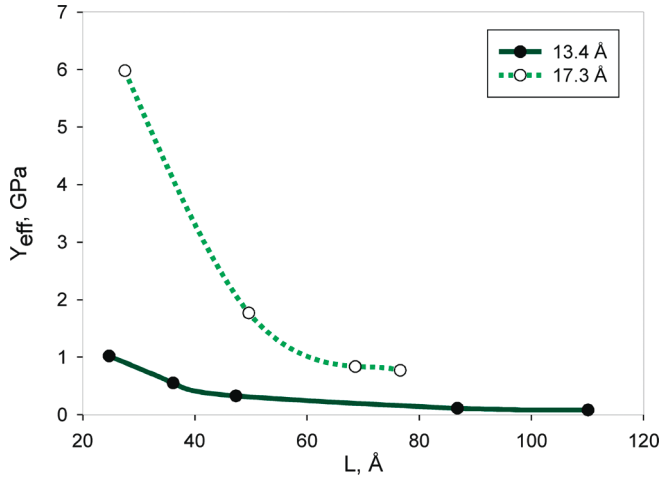

Figure 3. Effective Young's modulus (Y_{eff}) for Si−Y−NW as a function of branch length (L) of the nanowires. Two curves correspond to different nanowire diameters (13.4 and 17.3 Å).

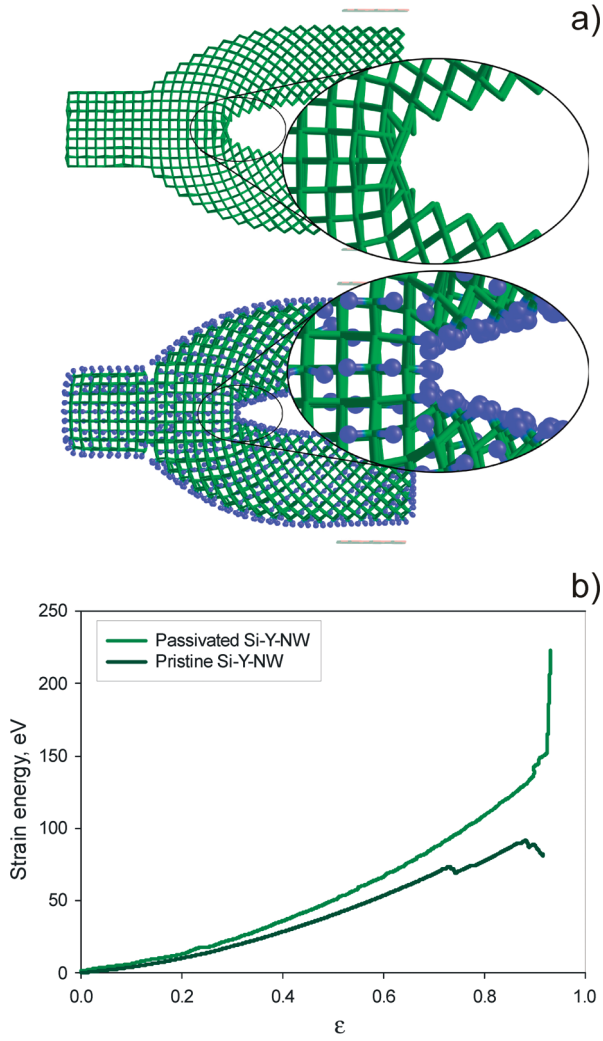

Figure 4. Comparison of passivated and unpassivated Si−Y−NW at ε = 0.78; the unpassivated Si−Y−NW bent inelastically due to the re-forming of the bonds in the region of branch crossing in the region $0.75 < \varepsilon < 0.88$, whereas the passivated Si−Y−NW bended elastically.

The bough three-terminal Si−YB−NW branched nanowire is formed by connection of a nanowire branch with the stem (Figure 1b). We used this type of clusters to model the structure of branched silicon nanowires obtained experimentally in the work of Wang *et al.*[9] (see Figure 1b, inset). It was shown that the stem is oriented along the $\langle\bar{1}11\rangle$ direction, whereas the branch is oriented along the $\langle\bar{1}1\bar{1}\rangle$ direction and was considered as a low-dimensional silicon monocrystal. To study the mechanical properties, we designed a number of finite branched Y-shaped bough-type nanowires with effective diameters of the stem and branches in the range of 1−2 nm. The Young moduli of the wires with longer branches were calculated using extrapolation of the data obtained for finite systems.

RESULTS AND DISCUSSION

The changes in the total energy with respect to the total energy of the initial strain-free configuration reflect the strain energy E as a function of strain ε. We estimated the effective Young modulus of the Y-shaped nanowire as $Y_{eff} = E''/r_0S$, where strain energy E was approximated as $E = 1/2E''\varepsilon^2$ on the assumption that the loading was mainly created by the atoms of the atomic plane and S is the square of the plane ($S = S_{fragment}$). The strain energy $E(\varepsilon)$ for the Y fork NW ($d =$ 17.3 Å, $L =$ 49.6 Å, Figure 2a) displays a quadratic behavior until $\varepsilon = 0.75$. Increasing the pressure leads to increased bond lengths between Si atoms at the outer wire surface region (the bonds are marked in blue, Figure 2c−e) and shortened ones in the inner surface region (the bonds are marked in red), with visible deflection of the bond angles from their natural tetrahedral value of 109.471° (compare panels b and c in Figure 2). The region of the main distortion of the crystalline structure is the branch crossing interface. Further increasing of the tension leads to re-forming of chemical bonds in the region of branch crossing ($\varepsilon \geq \varepsilon_{critical}$, Figure 2d) and formation of new bonds between the branch ends ($\varepsilon \geq \varepsilon'_{critical}$, Figure 2e) along with decreasing of the strain energy. The formation of new bonds between chemically active surface silicon atoms of different branches is energetically favorable; therefore, the whole energy of the structure goes down. Chemical passivation of the surface (*e.g.*, by hydrogen atoms) leads to disappearance of the effect. The study of the fork Si−Y−NW with passivated surface is given below.

The unloading of the wire in the region $\varepsilon'_{critical} > \varepsilon > \varepsilon_{critical}$ leads to unbending of the wire to a new structure with re-formed bonds in the region of branch crossing with slightly higher energy than the initial structure ($\Delta E \approx 3$ eV) and larger effective Young modulus (1.9 GPa, compare with 1.8 GPa). This effect can be used for hardening of the Y wires. For Y-shaped fork nanowires, the elastic data ($\varepsilon_{critical}$, $\varepsilon'_{critical}$, E'', Y_{eff}, E''/r_0) is presented in Table 1.

Increasing of the length of the branches from 24.7 to 110.1 Å (d = 13.4 Å) and from 27.5 to 76.6 Å (d = 17.3 Å) leads to decreasing of the effective Young modulus from 1.02 to 0.08 GPa and from 5.98 to 0.77 GPa, respectively (Figure 3). Due to decreasing of the relative number of distorted bonds and bond angles, the effective Young modulus of the wires with longer branches cannot be larger than for the studied systems.

The increasing of the length leads to increasing of pressured surface, but the size of the bending region located near the origin of the branches practically does not change. Actually, it can be treated as an increasing of the force arm acting to the branch. In its turn, this leads to the decreasing of the stiffness of the wire along with the decreasing of the effective Young's modulus.

The unpassivated surface of the wire can influence the mechanical behavior especially at the critical bending values. We studied the Si−Y−NW (L = 49.6 Å, d = 17.3 Å) with the passivated surface by hydrogen atoms. We studied the bending process of the wire and found that, due to the low chemical activity of hydrogen atoms, the branches of the wire do not bond with each other at the final deformation stage ($\varepsilon > \varepsilon_{critical}$, Figure 4a), and therefore, the strain energy of the passivated wire does not fall down and the energy moves up (Figure 4b). Also, the presence of hydrogen atoms increases the Si−Y−NW effective Young modulus (Y_{eff} = 2.58 GPa for passivated Si−Y−NW and 1.84 GPa for unpassivated Si−Y−NW) due to the interaction of neighboring hydrogen atoms during the bending.

Other types of passivation (*e.g.*, silicon nanowires obtained in experiments are usually coated by an amorphous SiO_x layer[16]) should also increase the nanowires' stiffness. The Young's modulus for such a coaxial wire depends on both wire effective diameter and thickness of the SiO_x layer. In its turn, the increasing of the SiO_x layer thickness increases the effective modulus of the wire. Such effect was observed in the case of the SiC−SiO_x coaxial nanocable.[17]

The unloading of elastically bent wires leads to oscillations of the branches with frequency depending on the wire size. We studied the oscillation of Si−Y−NW with various branch lengths and diameters (d = 12.7 Å, L = 52.9, 74.1, 84.6 Å; d = 13.4 Å, L = 47.5, 57.8 Å; d = 17.3 Å, L = 54.8, 76.5 Å) at a temperature of 300 K. The molecular dynamics simulation was carried out with a time step of 1 fs during 1 ns. The inner part of the Si−Y−NW stem was fixed. Using the dependence of atomic coordinates upon the time, frequencies of the branch oscillation were obtained.

The result of simulation of the frequency upon the dimensionless ratio $\delta = L/d$ is presented in Figure 5. The dependence can be useful to obtain the frequency value for any Si−Y−NW. The obtained data are well fitted by equation $\nu = a/\delta^b$, where a = 226.3 GHz and b = 1.823. The reasonability of the fitted equation is proved by reference experimental results; for example,

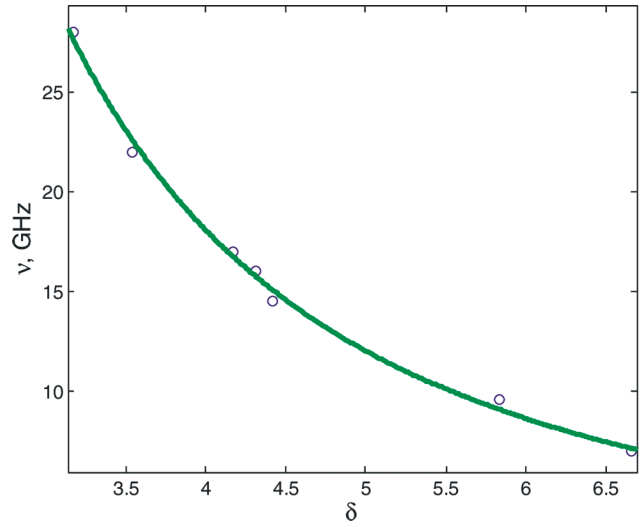

Figure 5. Dependence of branch oscillation frequency of Si−Y−NW upon the $\delta = L/d$ ratio.

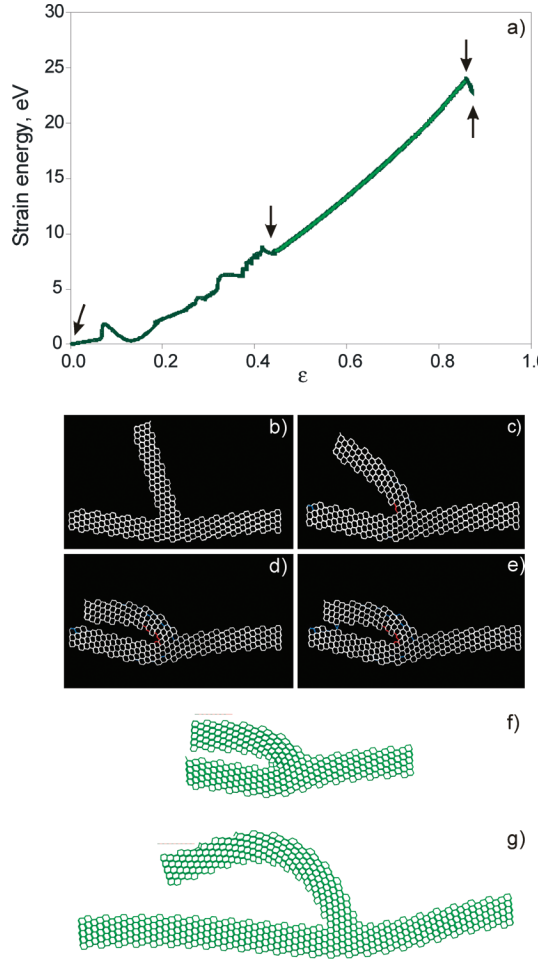

Figure 6. Behavior of a Si−NW bough junction under loading (a) strain energy of the Si−YB−NW (d = 13.5 Å, L = 57.9 Å) as a function of deformation ε. The arrows correspond to the stages of wire compression: (b) unstrained configuration (ε = 0); (c) ε = 0.44; (d) ε = 0.870 before the bonding; and (e) $\varepsilon_{critical}$ = 0.875 after the bonding of the branch and stem. The bonds shown in red have a length less than 2.26 Å, and the bonds shown in blue are larger than 2.41 Å (the Si−Si bond length in bulk silicon is equal to 2.3516 Å). The comparison between bending behavior of nanowires (ε = 0.85, d = 18.8 Å) with (f) short (L = 60.7 Å) and (g) long (L = 120.7 Å) branch lengths.

TABLE 2. Elastic Properties of Studied Si−YB−NW[a]

d, Å	*L*, Å	L_{stem}, Å	$\varepsilon_{critical}$	E'', eV	Y_{eff}, GPa	E''/r_0, eV/Å
9.5	45.1	103.4	0.77	30.55	0.49	0.81
	66.4	146.4	0.84	30.32	0.28	0.47
	107.2	194.9	0.77	36.23	0.22	0.36
13.5	38.6	93.5	0.66	136.45	2.45	4.08
	57.9	134.2	0.87	43.49	0.53	0.88
	86.6	134.7	0.69	26.74	0.19	0.32
	117.4	202.3	0.78	25.54	0.14	0.24
18.8	44.7	124.5	0.75	245.53	4.26	7.10
	60.7	124.5	0.90	126.90	1.38	2.30
	92.2	213.5	0.85	63.31	0.45	0.75
	120.7	233.5	0.75	59.66	0.32	0.53

[a]The *d* and *L* are the wire's branch diameter and length, respectively; L_{stem} is the length of the NW stem; and $\varepsilon_{critical}$ is critical strain to form new chemical bonds between the branch and the stem.

fundamental frequency of the silicon nanowire resonator,[18] $d = 30$ nm, $L = 1.8$ μm) is 75 MHz, whereas the fitted equation gives the 129 MHz for the Si−Y−NW with the same geometric parameters of the branches.

To study the effective Young modulus of the Y-shaped bough-type nanowires (Si−YB−NWs, Figure 1b), we calculated the structures with diameters of 9.5, 13.5, and 18.8 Å. To load the stress, the atomic plane was driven toward the single wire branch approaching the stem. Both ends of the stem were fixed. In Figure 6a−e, the results of applying of the external stress to the typical Si−YB−NW with $d = 13.5$ Å and $L = 57.9$ Å are presented. The mechanism of deformation of the Si−YB−NW junctions is more complex than the fork one. At the first stages of bending, the deformations of both branch and stem occur. Along with the bending of the branch, the stem buckles. This leads to oscillation of the strain energy (Figure 6a) in the region of $0 < \varepsilon < 0.44$. Pure bending of the branch begins from $\varepsilon = 0.44$ (Figure 6c) up to $\varepsilon_{critical} = 0.87$ (Figure 6d,a, light green part of the curve). Further increasing of the tension leads to re-formation of the bonds in the region of branch and stem crossing and formation of new covalent bonds between branch end and the stem (Figure 6e) with decreasing of the strain energy (Figure 6a). In the case of Si−YB−NWs with longer branch lengths, a deformation of only the branch part, located far away from the branch−stem crossing, occurs (Figure 6f,g). This effect is caused by irregular stiffness of the Si−YB−NWs.

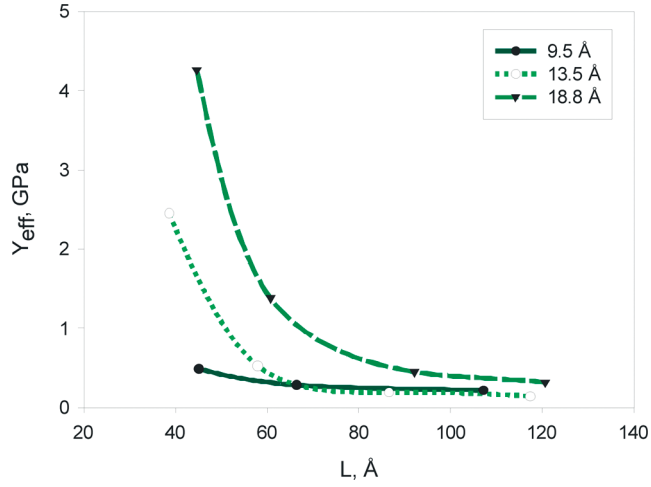

Figure 7. Effective Young's Modulus (Y_{eff}) for Si−YB−NWs as a function of branch length (*L*) of the nanowires. Three curves correspond to different nanowires diameters (9.5, 13.5, and 18.8 Å).

TABLE 3. Elastic Properties of Single-Walled and Double-Walled (Y-DWNT) Carbon Nanotube Bough Y-Junction (from ref 19)

	(*n*,*m*)-(*l*,*k*)	*d*, Å	*L*, Å	E'', eV	Y_{eff}, GPa	E''/r_0, eV/Å
Y-SWNT	(10,0)-(4,4)	5.4	45.0	14	1.09	0.44
	(19,0)-(9,9)	12.2	45.0	38	0.60	0.24
	(19,0)-(9,9)	12.2	90.0	34	0.30	0.12
Y-DWNT	(10,0)-(4,4)@(19,0)-(9,9)	12.2	90.0	46	0.40	0.16

The results of the calculation of effective Young modulus of Si−YB−NWs are presented in Figure 7. The elongation of the branches from 45.1 to 107.2 Å ($d = 9.5$ Å), from 38.6 to 117.4 Å ($d = 13.5$ Å), and from 44.7 to 120.7 Å ($d = 18.8$ Å) leads to decreasing of the Young modulus from 0.49 to 0.22 GPa, from 2.45 to 0.14 GPa, and from 4.26 to 0.32 GPa, respectively. The Y-shaped bough-type nanowire elastic data are presented in Table 2.

In the work of ref 19, the effective Young's modulus of the bough-type Y-junction single-walled carbon nanotubes (Y-SWNT) was calculated. For the Y-type nanotubes ($L = 45$ and 90 Å, branch diameter $d = 12.2$ Å) and Si−YB−NW ($L = 45.1$ and 107.2 Å, $d = 9.5$ Å; see Figure 7 and Table 1), the E''/r_0 values are equal to 0.24 eV/Å (Y-SWNT, $L = 45$ Å), 0.12 eV/Å (Y-SWNT, $L = 90$ Å), 0.81 eV/Å (Si−YB−NW, $L = 45.1$ Å), and 0.36 eV/Å (Si−YB−NW, $L = 107.2$ Å), respectively. The E''/r_0 of the double-walled carbon nanotube Y-junction is slightly larger (0.16 eV/Å, for $L = 90$ Å) than ones for Y-SWNTs but is less than E''/r_0 of the corresponding wire (the nanotube junction elastic data[19] are represented in Table 3). This result is bounded with the atomic geometry of the structures. Nanotubes are hollow objects, whereas wires represent the crystalline nature.

The unloading of elastically bent wires leads to oscillations of branches with a frequency depending on branch lengths and diameters. Therefore, such structures can be used as tuning forks with ultrahigh frequencies. We should mention that studied nanowires can be elastically bent under strain up to $\varepsilon = 0.9$ similar to the carbon nanotubes' bough Y-junction[19] and can be used along with them as nanosprings.

CONCLUSIONS

The elastic properties of branched Y silicon nanowires of fork and bough types were studied by

means of molecular mechanics simulations using the Tersoff model potential, and the effective Young moduli were calculated. During bending in the inelastic regime, the formation of new bonds between different parts of the nanowires in the region of branch crossing was observed. The Si−YB−NWs demonstrate complex mechanisms of deformation under external stress due to the NW's stem buckling in the first steps of bending. Due to irregularity of the branch stiffness, the Young moduli and bending mechanisms of the Si−Y−NWs and Si−YB−NWs depend upon the branch lengths. The stiffness of the studied nanowires and nanotubes was compared with the literature. The Si−Y−NW and Si−YB−NW behave as springs up to contact of branches, in contrast to similar Y-junctions of carbon nanotubes. It was found that the stiffness of the wires is much larger due to the crystalline structure of the wires. The effective Young modulus of nanowires with longer branch lengths was estimated.

METHODS

The simulations were performed using molecular mechanics with Tersoff model potential.[20,21] The potential successfully describes the atomic structure of bulk silicon and silicon nanowires,[22] silicon surfaces,[23] point defects,[24] and their elastic properties.[25,26] Depending on the wire configuration, up to 10 000 atoms were involved in the simulations using the Broyden−Fletcher−Goldfarb−Shanno (BFGS)[27] optimization technique.

To simulate external pressure, we used the method of atomic plane[19,28] with frozen atomic plane fragment ($S_{fragment}$ = 200 Å^2) driven toward a branch in small steps. We used the same plane fragment for all studied structures for the correct comparison of obtained elastic data. We performed an optimization of the atomic structure of the entire wire at each single step. All studied wires were fixed in transversal direction. Some parts of the wires were also fixed to avoid a meaningless shaking of the structure, and the end/ends of the stem was/were fixed for the fork/bough-type nanowires. To calculate the NW's strain energy, we chose the pure repulsive potential between the plane and nanowire to avoid nonrealistic bonding between them. The bending strain was defined as $\varepsilon = \Delta r/r_0$, where $\Delta r = r_0 - r$; r_0 is the distance in unstrained structure between edge atoms of the branch ends of the fork NW or between the edge atoms of the end of the branch and the surface atoms of the stem of the bough NW, and r is the current distance (Figure 1).

Acknowledgment. P.B.S. acknowledges partial support by the National Science Foundation grant CMMI-0708096, NIRT. L.A.C. was supported by the Russian Academy of Sciences, program No. 21. P.V.A. and P.B.S. also acknowledge the collaborative RFBR-JSPS Grant No. 09-02-92107-ЯФ. All calculations have been performed on the Joint Supercomputer Center of the Russian Academy of Sciences. The geometry of all presented structures was visualized by ChemCraft software.

REFERENCES AND NOTES

1. Cui, Y.; Lieber, C. M. Functional Nanoscale Electronic Devices Assembled Using Silicon Nanowire Building Blocks. *Science* **2001**, *291*, 851–853.
2. Cui, Y.; Zhong, Z. H.; Wang, D. L.; Wang, W. U.; Lieber, C. M. High Performance Silicon Nanowire Field Effect Transistors. *Nano Lett.* **2003**, *3*, 149–152.
3. Huang, Y.; Duan, X.; Cui, Y.; Lauhon, L. J.; Kim, K.; Lieber, C. M. Logic Gates and Computation from Assembled Nanowire Building Blocks. *Science* **2001**, *294*, 1313–1317.
4. Cui, Y.; Wie, Q.; Park, H.; Lieber, C. M. Nanowire Nanosensors for Highly Sensitive and Selective Detection of Biological and Chemical Species. *Science* **2001**, *293*, 1289–1292.
5. Morales, A. M.; Lieber, C. M. A Laser Ablation Method for the Synthesis of Crystalline Semiconductor Nanowires. *Science* **1998**, *279*, 208–211.
6. Park, W. I.; Zheng, G.; Jiang, X.; Tian, B.; Lieber, C. M. Controlled Synthesis of Millimeter-Long Silicon Nanowires with Uniform Electronic Properties. *Nano Lett.* **2008**, *8*, 3004–3009.
7. Wang, D.; Lieber, C. M. Inorganic Materials: Nanocrystals Branch Out. *Nat. Mater.* **2003**, *2*, 355–356.
8. Fonseca, L. F.; Resto, O.; Sol, F. Electron-Beam-Induced Growth of Silicon Multibranched Nanostructures. *Appl. Phys. Lett.* **2005**, *87*, 113111(3).
9. Wang, D.; Qian, F.; Yang, C.; Zhong, Z.; Lieber, C. M. Rational Growth of Branched and Hyperbranched Nanowire Structures. *Nano Lett.* **2004**, *4*, 871–874.
10. Kanaras, A.G.; Sönnichsen, C.; Liu, H.; Alivisatos, P. Controlled Synthesis of Hyperbranched Inorganic Nanocrystals with Rich Three-Dimensional Structures. *Nano Lett.* **2005**, *5*, 2164–2167.
11. Menon, M.; Richter, E.; Lee, I.; Raghavan, P. Si-Nanotrees: Structure and Electronic Properties. *J. Comp. Theor. Nanosci.* **2007**, *4*, 252–256.
12. Avramov, P. V.; Chernozatonskii, L. A.; Sorokin, P. B.; Gordon, M. S. Multiterminal Nanowire Junctions of Silicon: A Theoretical Prediction of Atomic Structure and Electronic Properties. *Nano Lett.* **2007**, *7*, 2063–2067.
13. Leu, P. W.; Svizhenko, A.; Cho, K. *Ab Initio* Calculations of the Mechanical and Electronic Properties of Strained Si Nanowires. *Phys. Rev. B* **2008**, *77*, 235305(14).
14. Lee, B.; Rudd, R. E. First-Principles Study of the Young'S Modulus of Si <001> Nanowires. *Phys. Rev. B* **2007**, *75*, 041305(R).
15. Wyckoff, R. W. G. *Crystal Structures*; John Wiley & Sons: New York, 1963; Vol. 1.
16. Hu, J.; Odom, T. W.; Lieber, C. M. Chemistry and Physics in One Dimension: Synthesis and Properties of Nanowires and Nanotubes. *Acc. Chem. Res.* **1999**, *32*, 435–445.
17. Wang, Z. L. Mechanic Properties of Nanowires and Nanobelts. In *Dekker Encyclopedia of Nanoscience and Nanotechnology*; Schwarz, J. A., Contescu, C. I., Putyera, P. , Eds.; Taylor & Francis: London, 2004; pp 1773−1786.
18. He, R.; Feng, X. L.; Roukes, M. L.; Yang, P. Self-Transducing Silicon Nanowire Electromechanical Systems at Room Temperature. *Nano Lett.* **2008**, *8*, 1756–1761.
19. Belova, E.; Chernozatonskii, L. A. Mechanical Properties of Carbon Nanotube Bough Junctions: A Theoretical Study. *Phys. Rev. B* **2007**, *75*, 073412(4).
20. Tersoff, J. Empirical Interatomic Potential for Silicon with Improved Elastic Properties. *Phys. Rev. B* **1988**, *38*, 9902–9905.
21. de Brito Mota, F.; Justo, J. F.; Fazzio, A. Hydrogen Role on the Properties of Amorphous Silicon Nitride. *J. Appl. Phys.* **1999**, *86*, 1843–1847.
22. Zhao, Y.; Yakobson, B. I. What is the Ground-State Structure of the Thinnest Si Nanowires? *Phys. Rev. Lett.* **2003**, *91*, 035501(4).
23. Liu, W.; Zhang, K.; Xiao, H.; Meng, L.; Li, J.; Stocks, G. M.; Zhong, J. Surface Reconstruction and Core Distortion of Silicon and Germanium Nanowires. *Nanotechnology* **2007**, *18*, 215703(9).
24. Posselt, M.; Gao, F.; Bracht, H. Correlation between Self-Diffusion in Si and the Migration Mechanisms of Vacancies and Self-Interstitials: An Atomistic Study. *Phys. Rev. B* **2008**, *78*, 035208(9).

25. Zhu, R.; Pan, E.; Chung, P. W.; Cai, X.; Liew, K. M.; Buldum, A. Atomistic Calculation of Elastic Moduli in Strained Silicon. *Semicond. Sci. Technol.* **2006**, *21*, 906–911.
26. Kim, T. Y.; Han, S. S.; Lee, H. M. Nanomechanical Behavior of β-SiC Nanowire in Tension: Molecular Dynamics Simulations. *Mater. Trans.* **2004**, *45*, 1442–1449.
27. Press, W. H.; Teukolsky, S. A.; Vetterling, W. T.; Flannery, B. P. *Numerical Recipes*, 2nd ed.; Cambridge University Press: Cambridge, 1992.
28. Chernozatonskii, L. A.; Ponomareva, I. V. Sticking of Carbon Nanotube Y Junction Branches. *JETP Lett.* **2003**, *78*, 327–331.